Research Article

Long-Term Assessment of Cattail (*Typha spp.*) Dynamics and Wetland Restoration in the Everglades Using Object-Based Landsat Time Series and Markov Modeling

Gideon Tandoh [1], Stephen Yankyera [2,*], and Michael Sean Chenoweth [1]

[1] Department of Chemistry and Geosciences, Geographic Research and Information Laboratory, Jacksonville State University, Jacksonville, AL 36265, USA, gtandoh@stu.jsu.edu, mchenoweth@jsu.edu

[2] Department of Geography and Planning, Spatially Integrated Social Science Ph.D. Program, The University of Toledo, Toledo, Ohio 43606, USA, stephen.yankyera@rockets.utoledo.edu

* Corresponding Author: email; stephen.yankyera@rockets.utoledo.edu , +1 (614)-307-6884

Academic Editor: Jeong Chang Seong
Received: 19 February 2026
Revised: 25 March 2026
Accepted: 26 March 2026
Published: 8 April 2026

Copyright: © 2026 by the authors. Submitted for open access publication under the terms and conditions of the Creative Commons Attribution (CC BY) license (https:// creativecommons.org/ licenses/by/4.0/).

Abstract: Assessing long-term vegetation response to restoration requires spatially consistent monitoring approaches that capture both observed change and likely future trajectories. In the Florida Everglades, nutrient enrichment contributed to the expansion of cattail (*Typha spp.*) within Water Conservation Area 3A (WCA-3A), raising concerns about restoration effectiveness. This study integrates a multi-temporal Landsat time series (2004–2024), object-based image analysis (OBIA), support vector machine (SVM) classification, and Markov transition modeling to quantify and project vegetation change in WCA-3A. Object-based segmentation reduced classification fragmentation in heterogeneous marsh landscapes, while SVM improved separation among spectrally similar vegetation classes. Classification accuracies remained consistently high across sensors (overall accuracy 90–93%; kappa 0.80–0.87). Cattail cover peaked at over 11% in the late 2000s but declined to 1.6% by 2024, coinciding with the expansion of native sawgrass and open marsh communities. Transition probabilities derived from object-level change detection were used to project vegetation patterns to 2034 under continued management conditions, indicating sustained suppression of cattail dominance if current controls persist. By directly linking object-based classification with probabilistic forecasting, this study advances beyond static land-cover mapping and provides a transferable framework for evaluating restoration trajectories in large managed wetlands.

Keywords: *Typha*, Landsat time series, object-based image analysis, support vector machine, Markov modeling

1. Introduction

Wetlands are critical components of the Earth system, which regulate water flow, retain nutrients, store carbon, and support diverse plant and animal communities (Yankyera and Alam, 2025; Sandhya et al., 2025). Despite their ecological importance, wetlands are highly sensitive to changes in hydrology and nutrient inputs. Even moderate shifts in water levels or phosphorus concentrations can alter vegetation structure and lead to long-term changes in ecosystem composition (Reis et al., 2017; Cui et al., 2021). Because many large wetland systems are actively managed, consistent long-term monitoring is necessary to understand how vegetation responds to both disturbance and restoration.

Citation: Tandoh, G., Yankyera, S., & Chenoweth, M.S. (2026). Long-Term Assessment of Cattail (Typha spp.) Dynamics and Wetland Restoration in the Everglades Using Object-Based Landsat Time Series and Markov Modeling. Journal of Earth Observation and Geospatial Applications, 2(2), 1–20. DOI: https://doi.org/10.65372/rd89px81

The Florida Everglades is one of the largest managed wetland systems in the world. Over the past century, drainage canals, levees, and agricultural runoff have altered natural flow patterns and increased phosphorus concentrations across parts of the system (Willard and Bernhardt, 2011; Finkl and Makowski, 2017). In Water Conservation Area 3A (WCA-3A), a 198,727-ha freshwater marsh south of Lake Okeechobee, these alterations contributed to substantial shifts in vegetation structure. Areas historically dominated by sawgrass (*Cladium jamaicense*) experienced expansion of cattail (*Typha spp.*) beginning in the 1970s, particularly in nutrient-enriched zones (Belanger et al., 2009; Entry and Gottlieb, 2014). Although *Typha* is native to Florida,

elevated phosphorus levels enabled it to expand beyond its historical distribution, forming dense stands that replaced mixed marsh communities and modified habitat structure and ecosystem processes (Lagerwall et al., 2012).

In response, the Comprehensive Everglades Restoration Plan (CERP) was initiated in 2000 to improve water quality and restore more natural hydrological conditions. In practice, nutrient reduction has been achieved through the construction and operation of stormwater treatment areas (STAs), which remove phosphorus from agricultural runoff before it enters marsh systems, alongside agricultural and urban best management practices (BMPs) that reduce nutrient inputs at the source. Concurrently, hydrologic adjustments have involved modifications to water delivery, storage, and flow regulation to better approximate natural hydroperiods and sheet flow patterns across the Everglades landscape (South Florida Water Management District [SFWMD], n.d.; South Florida Ecosystem Restoration Task Force, n.d.). A key question in WCA-3A is whether these restoration-driven nutrient reductions and hydrologic adjustments have contributed to slowing or reversing cattail dominance. Addressing this question requires spatially consistent vegetation information across multiple decades. While satellite imagery has been used to map vegetation patterns in portions of the Everglades (Belanger et al., 2009; Zhang et al., 2017), long-term assessments focused specifically on WCA-3A using object-based approaches remain limited. This limits the ability to evaluate restoration outcomes in a spatially explicit manner. Invasive plant monitoring in wetlands has increasingly relied on satellite-based observations to quantify spatial extent, track expansion patterns, and evaluate management outcomes. Previous studies have demonstrated the utility of Landsat and other medium-resolution imagery for detecting large-scale shifts in dominant vegetation types, including cattail expansion in nutrient-enriched marsh systems (Belanger et al., 2009; Zhang et al., 2017). However, accurately distinguishing invasive stands from structurally similar native communities remains challenging in heterogeneous wetlands. This has motivated the adoption of object-based and machine learning approaches to improve classification stability and reduce fragmentation in marsh landscapes. Despite these advances, relatively few studies have integrated object-level change detection with predictive transition modeling to assess restoration trajectories over multi-decadal periods.

The Landsat archive provides a practical foundation for multi-decadal monitoring. Its continuous coverage enables consistent observation of vegetation dynamics over time. However, wetland landscapes are often characterized by fine-scale patchiness and mixed plant assemblages, which can reduce the reliability of pixel-based classification methods. Such approaches frequently produce fragmented outputs in marsh environments. Object-based image analysis (OBIA) addresses this limitation by grouping adjacent pixels into meaningful segments prior to classification, allowing spatial context and texture to be incorporated alongside spectral information (Blaschke, 2010; Lu and Weng, 2007). When combined with support vector machine (SVM) classifiers, which are effective in separating spectrally similar vegetation types (Pal and Mather, 2005; Mountrakis et al., 2011), object-based methods can improve classification stability in heterogeneous wetland systems (Hestir et al., 2008; Wang et al., 2022).

Beyond documenting past change, restoration planning also requires insight into likely near-term vegetation trajectories. Markov chain models estimate transition probabilities among land-cover classes based on observed temporal dynamics and can be used to project future landscape conditions under prevailing trends (Stepchenko and Chizhov, 2015). Although these models assume stationary transition probabilities, they provide a practical mechanism for linking empirical change detection with forward-looking assessment.

This study uses a multi-temporal Landsat time series from 2004 to 2024 to evaluate vegetation change in WCA-3A through object-based segmentation and SVM classification. The results quantify shifts in major plant communities, with particular attention to *Typha spp.*, and derive transition probabilities to project vegetation patterns to 2034 under continued management conditions. The study integrates long-term Earth observation with transition-based modeling, which supports spatially explicit evaluation of vegetation dynamics and restoration outcomes in a managed wetland system.

2. Study Area and Methods

2.1. Study Area

WCA-3A is a vast freshwater marsh in southern Florida, comprising the western portion of the greater Everglades Water Conservation Area 3 (Figure 1). Bounded by canals and levees, it receives regulated inflows from the north and drains southward toward Everglades National Park. The area has a tropical monsoon

climate with pronounced wet (summer) and dry (winter) seasons, which drive annual flooding and drying cycles in the marsh. Under pre-drainage conditions, WCA-3A's landscape was dominated by *Cladium jamaicense* (sawgrass) prairies interspersed with open-water sloughs and tree islands. Today, sawgrass remains the prevalent native cover, especially in northern and central WCA-3A (Yeoman et al., 2017). Other native communities include open marsh (emergent broadleaf aquatics and wet prairie assemblages, often more extensive in the south/southwest) and shrubland (woody species like coastal willow and wax myrtle, concentrated along the slightly higher eastern boundary) (Yeoman et al., 2017). These vegetation patterns reflect underlying hydrological and nutrient gradients across the area.

WCA-3A has also been invaded by cattail (*Typha spp.*), which became established in nutrient-enriched zones and can form dense monocultures in shallow water. By the early 2000s, cattail patches were relatively small and mostly confined to the eastern and western fringes and a few northern pockets of WCA-3A (near canal inflows). Resource managers are concerned about cattail's potential to expand and displace sawgrass, as occurred in some other Everglades regions when phosphorus levels rose in the 1990s (Lagerwall et al., 2012). The ecological significance of WCA-3A and its vulnerability to invasion make it a high priority for monitoring and restoration. Moreover, WCA-3A is a keystone in regional water management. It not only supports habitat for threatened Everglades fauna but also helps regulate flood control and water supply for South Florida (Davis and Ogden, 1994). Understanding vegetation changes here is therefore vital for both biodiversity conservation and hydrological restoration goals.

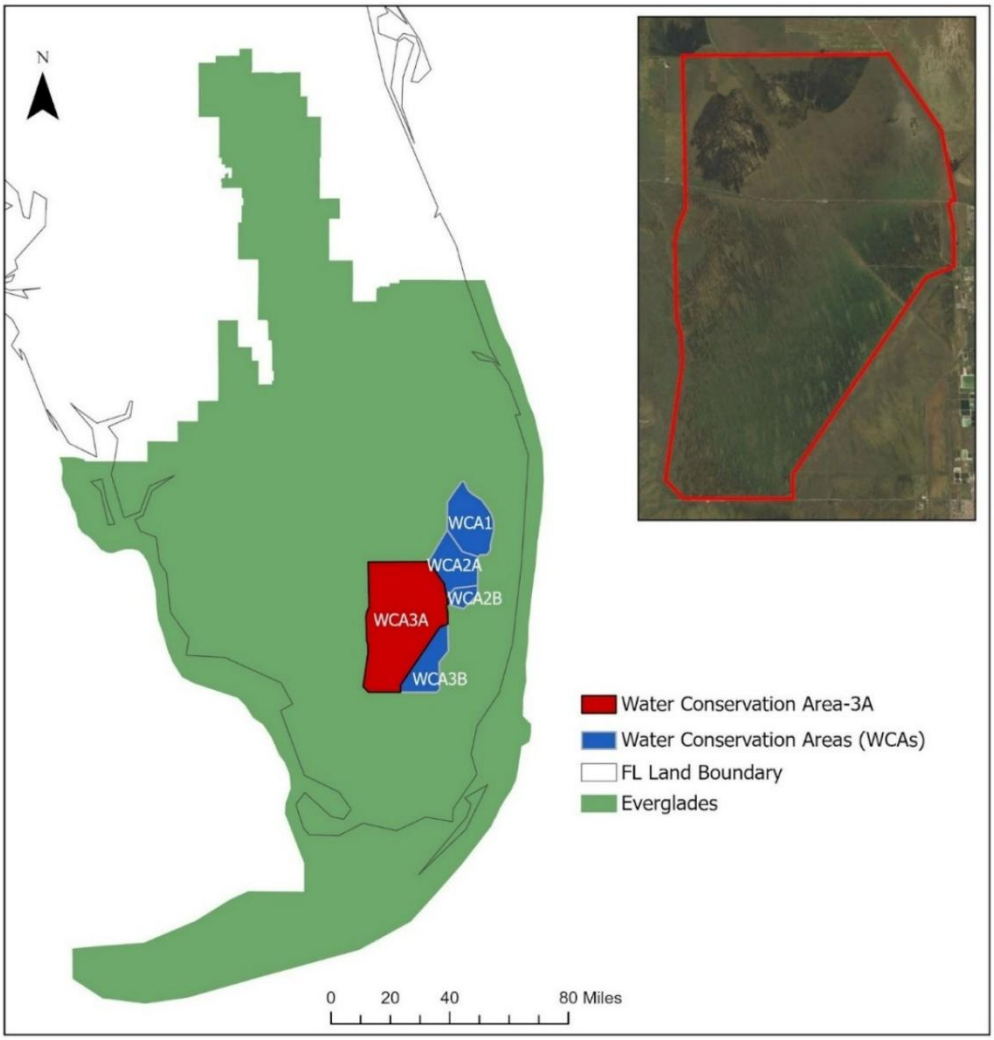

Figure 1. Study area map showing the location of Water Conservation Area 3A (WCA-3A) within the Florida Everglades.

2.2. Data

This study utilized Landsat satellite images from the USGS EarthExplorer website to map WCA-3A's vegetation over 20 years. Five mostly cloud-free scenes were selected at approximately four-year intervals from 2004 to 2024, all captured in the late dry season to ensure consistent phenological conditions. The images (Table 1) were acquired on the following dates, as shown in the table.

Table 1. Summary of Landsat satellite data used for time-series vegetation mapping (2004–2024).

Date	Dataset	Data Source	Spatial Resolution	Bands used
23 Jan 2004	Landsat C2 Level-2	Landsat-5 TM	30m	1–5 and 7
23 Apr 2008	Landsat C2 Level-2	Landsat-5 TM	30m	1–5 and 7
23 Mar 2014	Landsat C2 Level-2	Landsat-8 OLI	30m	2–7
19 Apr 2018	Landsat C2 Level-2	Landsat-8 OLI	30m	2–7
07 Feb 2024	Landsat C2 Level-2	Landsat-9 OLI	30m	2–7

To have accurate and reliable results, we only utilized images that had less than 3% cloud cover. The few cloud or cloud-shadow pixels present (mostly in the 2008, 2014, and 2018 scenes) were masked out during preprocessing (Figure 2) and clipped to the WCA-3A boundary before analysis. Since the data were in Landsat C2 Level-2, further processing was not needed before the classification (Yankyera and Alam, 2025). In addition to the Landsat imagery, a high-resolution vegetation map of WCA-3A from 2004, produced by the South Florida Water Management District (SFWMD), was used as ancillary data. This 2004 vector map provided a baseline classification of plant communities in WCA-3A, against which our 2004 Landsat-based classification could be calibrated. It also guided training sample selection (Figure 2) by identifying known locations of each vegetation type in the initial year. For validation purposes, we compiled historical field reports and higher-resolution imagery (e.g., Google Earth and aerial photos) to help verify classification accuracy in various parts of WCA-3A, especially for the later years where ground truth data were limited.

2.3. Methods

2.3.1. Image Preprocessing

Each Landsat image was preprocessed to maximize consistency across dates and sensor types. First, cloud masking was applied using the Quality Assessment (QA) bands included with the Landsat surface reflectance products. All pixels flagged as clouds or cloud shadows in the QA mask were removed from the analysis. Because the selected images had very low cloud coverage (2% or less), masking eliminated only a small number of pixels and had minimal impact on data availability, while preventing potential classification errors in those areas. Figure A1 (Appendix A) shows the natural color (RGB) composites of all Landsat scenes used in the time series.

After cloud and shadow masking, we performed radiometric normalization to correct for sensor differences and subtle atmospheric effects between image dates (Appendix A, Table A1). The 2004 Landsat-5 TM scene was chosen as the reference baseline. All other images (2008–2024) were adjusted to match the 2004 reflectance scale using a pseudo-invariant feature (PIF) regression approach. Specifically, we identified a set of 28–32 PIFs in each image, areas assumed to have stable reflectance over time, such as deep-water bodies, bare ground, and certain infrastructure. For each image year, we performed ordinary least-squares regression between the reflectance values of the PIF pixels in that image (Appendix A, Figure A2) and the corresponding pixels in the 2004 reference image, on a band-by-band basis.

The results of the linear regression equations were then used to transform the image's pixel values to the 2004 reference scale. This procedure effectively aligned the multi-temporal imagery to a common radiometric baseline. This ensured that observed spectral differences between years were due to land cover change rather than sensor or atmospheric discrepancies. The strong correlations ($R^2 \approx 0.71$–0.93) observed in scatterplots of 2004 against other-year PIF reflectance (Appendix A, Figure A2) confirmed the validity of the normalization. Following normalization, all images were clipped to the exact WCA-3A boundary and assembled into the time-series dataset for analysis.

2.3.2. Object-Based Segmentation

We applied multiresolution mean-shift segmentation in ArcGIS Pro to partition each Landsat scene into

spatially homogeneous objects before classification. Segmentation was performed using the six reflective Landsat bands (Blue, Green, Red, Near-infrared (NIR), SWIR1, and SWIR2) to ensure that both vegetation vigor and moisture gradients were incorporated into object delineation. Segmentation parameters were calibrated using the 2004 image and the South Florida Water Management District vegetation reference map to ensure that resulting objects corresponded to meaningful landscape patches (e.g., sawgrass marshes, cattail stands, tree islands, and open water sloughs). This object-based framework reduces within-class spectral variability and mitigates the salt-and-pepper effect commonly associated with pixel-level wetland classifications (Blaschke, 2010).

Segmentation was implemented using ArcGIS Pro's Segment Mean Shift tool. Final parameters were held constant across all time steps to maintain temporal comparability: spectral detail = 15.50, spatial detail = 16, and minimum segment size = 20 pixels. At 30m spatial resolution, a minimum segment size of 20 pixels corresponds to approximately 1.8 ha, aligning with the characteristic scale of marsh vegetation patches in WCA-3A. These values were selected after iterative testing against the 2004 reference vegetation map and high-resolution imagery to balance over-segmentation in homogeneous marsh areas with under-segmentation of narrow cattail patches and tree island margins. The resulting segments corresponded to vegetation patches on the order of several hectares, consistent with the dominant structural scale of WCA-3A marsh communities.

Several test runs were conducted during parameter calibration. Segment outputs were visually inspected against reference imagery to confirm that dominant vegetation patches were delineated coherently while minimizing excessive fragmentation. By operating on image objects rather than individual pixels, the classification focused on ecologically meaningful landscape units and reduced spectral noise within heterogeneous marsh mosaics. This approach improves class stability across dates and enhances discrimination among spectrally similar vegetation types in large wetland systems.

2.3.3. Classification Scheme and Training Data

We defined five land cover classes for mapping WCA-3A: Sawgrass, Open Marsh, Shrubland, Cattail, and Others. Sawgrass denotes areas dominated by sawgrass *(Cladium jamaicense)*; Open Marsh includes various non-woody marsh vegetation and open water/emergent mix (e.g., spike rush, water lily sloughs); Shrubland covers woody vegetation (primarily stands of willow, bayhead, or wax myrtle); Cattail refers specifically to stands of *Typha spp.* (whether monotypic or mixed with other emergents); and Others is a minor catch-all category for features like levees, roads, or bare ground that occupy very small portions of WCA-3A. This classification scheme was informed by the 2004 SFWMD vegetation map, which indicated these as the major cover types present in the area. *Typha spp.* were the primary invasive plant of interest in our study, whereas other invasive plants (e.g., Melaleuca trees) were largely absent or already significantly reduced by the 2000s and thus were not mapped as separate classes (Rodgers et al., 2018).

To train the classifier, we adopted a hybrid sampling strategy leveraging both the 2004 reference map and a temporal change detection approach. For the 2004 image, we extracted training samples directly from the SFWMD 2004 vegetation map: polygons of known sawgrass, cattail, etc., were overlaid on the Landsat image, and the corresponding segments were labeled as training examples of their respective classes. This provided a high-confidence training set for the base year. For the subsequent years (2008–2024), when no independent field classification was available, we employed an iterative self-training approach using multi-temporal NDVI (normalized difference vegetation index) stability. We computed NDVI for each image date and generated NDVI difference images between consecutive time steps. Segments that showed minimal NDVI change over multiple intervals (i.e., likely unchanged areas of stable vegetation) were assumed to retain the same class over time. Using these unchanged segments as "anchor" points, we assigned them the same class label as in the nearest earlier map. For example, if a particular segment was classified as sawgrass in 2008 and exhibited negligible NDVI change through 2014, we included it as a sawgrass training sample for 2014 as well.

This object-based temporal sampling ensured consistency of training data across the time series and focused on clear cases of persistence to train the classifier. Additional training segments were selected manually by on-screen interpretation of each image, especially for areas where new cattail patches emerged or where cattail had visibly receded. In total, a few hundred training segments per class were used for each date. Care was taken to distribute training sites across WCA-3A's spatial extent and to include segments of various sizes and landscape positions (interior marsh vs. near canals, etc.), so that the classifier would generalize well across the whole area.

2.3.4. SVM Classification and Accuracy Assessment

Following segmentation, vegetation classes were assigned using a SVM classifier with a radial basis function (RBF) kernel implemented in ArcGIS Pro. SVM was selected due to its ability to model non-linear class boundaries and perform effectively in high-dimensional feature space, particularly in heterogeneous wetland environments (Mountrakis et al., 2011; Erfanifard et al., 2022; Kanjin and Alam, 2024). For each image date, mean spectral reflectance values from the six Landsat reflective bands (Blue, Green, Red, NIR, SWIR1, SWIR2) were extracted at the object level and used as predictor variables. The SVM was applied using the default RBF kernel configuration provided in ArcGIS Pro. Training samples were stratified by vegetation class and spatially distributed across WCA-3A to ensure representation of varying hydrological and nutrient conditions. Separate classification models were developed for each time step to account for spectral variability associated with sensor transitions (Landsat 5 TM, Landsat 8 OLI, Landsat 9 OLI) and interannual environmental differences.

Classification performance was evaluated using confusion matrix analysis. For each year, overall accuracy, producer's accuracy, user's accuracy, and kappa statistics were calculated based on independent validation samples. Validation data consisted of withheld object segments not used during model fitting, interpretation of high-resolution imagery (Google Earth and aerial photography), and, for 2004, comparison with the South Florida Water Management District (SFWMD) vegetation reference map. To ensure independence between training and validation data, validation segments were spatially distinct from training samples and were excluded from model fitting for each classification year. For years in which NDVI-based temporal stability was used to identify training anchors, those segments were not included in validation datasets. Accuracy metrics were therefore derived from independent object samples, minimizing bias in performance estimation. Detailed confusion matrices and class-specific accuracy statistics for all classification years are provided in Appendix A (Table A2).

2.3.5. Change Analysis

Once the series of vegetation maps (2004, 2008, 2014, 2018, 2024) was finalized, we conducted a post-classification change detection to quantify transitions among classes over time. For each consecutive interval (2004–2008, 2008–2014, 2014–2018, 2018–2024), we overlaid the classification maps and computed class-wise area changes and conversion matrices. The area of each class in each year is summarized in Table 4, and the gains/losses between years are given in Table 5. This analysis allowed us to identify which vegetation types were expanding or contracting in each period, and at what rates. We paid special attention to the invasive cattail class, mapping where cattail increased or decreased and measuring the net change in cattail coverage over the full 20-year span. We also examined the spatial distribution of changes using GIS, identifying "hotspots" of cattail expansion (for example, downstream of major canal inputs) or retreat (such as areas near active management or improved water flow). Because the classification intervals are uneven (ranging from 4–6 years apart), our change analysis focused on overall trends and multi-year shifts rather than precise annual rates. To contextualize the remote sensing findings, we noted the timeline of major restoration and management actions (e.g., the implementation of large Stormwater Treatment Areas and stricter nutrient controls around 2010–2015) and significant environmental events (hurricanes, droughts) that might explain observed changes during certain intervals.

2.3.6. Markov Chain Modeling

To extend the observed vegetation trajectories into a near-term projection, we implemented a first-order Markov chain model based on empirically derived class transitions between 2004 and 2024. A Markov process assumes that the probability of transitioning to a future state depends only on the current state. Formally, the transition probability is defined as:

$$P(X_{t+1} = j \mid X_t = i) = p_{ij} \tag{1}$$

where X_t represents the land-cover class at time t, X_{t+1} represents the class at the next time step, and p_{ij} denotes the probability that a pixel transitions from class i to class j. The full set of transition probabilities forms a transition matrix $P = [p_{ij}]$, where each row satisfies:

$$\sum_{j=1}^{n} p_{ij} = 1 \quad (2)$$

for each class i.

The transition matrix was derived through pixel-level post-classification comparison of the 2004 and 2024 vegetation maps. The 2004 map was treated as the initial state, and the 2024 map as the final state after one empirical time step of 20 years. By cross-tabulating class labels between these two maps, we computed the probability of each vegetation class transitioning to every other class over the 20-year interval. The resulting 5 × 5 transition matrix summarizes dominant vegetation conversion tendencies among Sawgrass, Open Marsh, Shrubland, Cattail, and Others.

Under the assumption that these transition probabilities remain broadly representative of near-term dynamics under continued restoration conditions, the matrix *P* was applied to the 2024 land-cover distribution to estimate projected class proportions for 2034. Because the empirical transition interval spans 20 years, the 2034 projection (a 10-year step) implicitly assumes proportional stability in transition tendencies over shorter periods. This stationarity assumption simplifies complex ecological processes but is reasonable given the relatively consistent nutrient management and hydrological restoration measures implemented during the study period.

To generate a spatially explicit forecast map, a CA-Markov approach was implemented in IDRISI Selva 17.00. The cellular automata (CA) component incorporated neighborhood context during class allocation using a 5 × 5 contiguity filter, ensuring that projected classes maintained spatial coherence consistent with observed landscape structure. No additional environmental suitability layers were introduced; therefore, the projection reflects continuation of empirically observed transition patterns rather than a mechanistic simulation driven by external covariates.

Model reliability was evaluated through a hindcasting procedure. Transition probabilities were first calculated using the 2004–2018 vegetation maps and applied to project class distribution for 2024. The projected 2024 map was then compared with the observed 2024 classification. Agreement was assessed using the kappa statistic. The overall kappa between predicted and observed 2024 maps was approximately 0.846, indicating strong agreement. A location-specific kappa of approximately 0.92 further demonstrated high spatial correspondence between predicted and observed class placement.

These validation results indicate that the Markov framework captures dominant transition tendencies at the decadal scale. However, the model assumes relative stability in transition probabilities and does not account for abrupt climatic events, extreme hydrological variability, or major policy shifts. The 2034 projection (a 10-year step) implicitly assumes proportional stability in transition tendencies. Because the empirical transition probabilities were derived from a 20-year interval (2004–2024), application to a 10-year forecast assumes proportional scaling of transition intensities over shorter durations. While this assumption simplifies potential non-linear ecological dynamics, it provides a transparent baseline for evaluating restoration trajectories under continued management conditions.

2.3.7. Methodological Workflow

The methodological workflow (Figure 2) integrated multi-temporal Landsat imagery (2004, 2008, 2014, 2018, and 2024) with object-based image analysis (OBIA), machine learning classification, and predictive modeling to assess vegetation dynamics in WCA-3A. Preprocessing involved cloud masking, radiometric normalization using PIFs, and NDVI computation to support stable training sample selection across years. Segmentation was performed via multiresolution mean-shift algorithms to generate spatially homogeneous objects, which were subsequently classified using a Support Vector Machine (SVM) with a RBF kernel, trained on a hybrid dataset combining reference map-derived samples (for 2004) and NDVI-based stable segments (for later years). Classification outputs were validated through accuracy assessments incorporating cross-validation and high-resolution imagery interpretation. Finally, a CA-Markov chain model was applied to derive transition probabilities from 2004–2024 change patterns and predict the vegetation distribution for 2034 under a business-as-usual scenario.

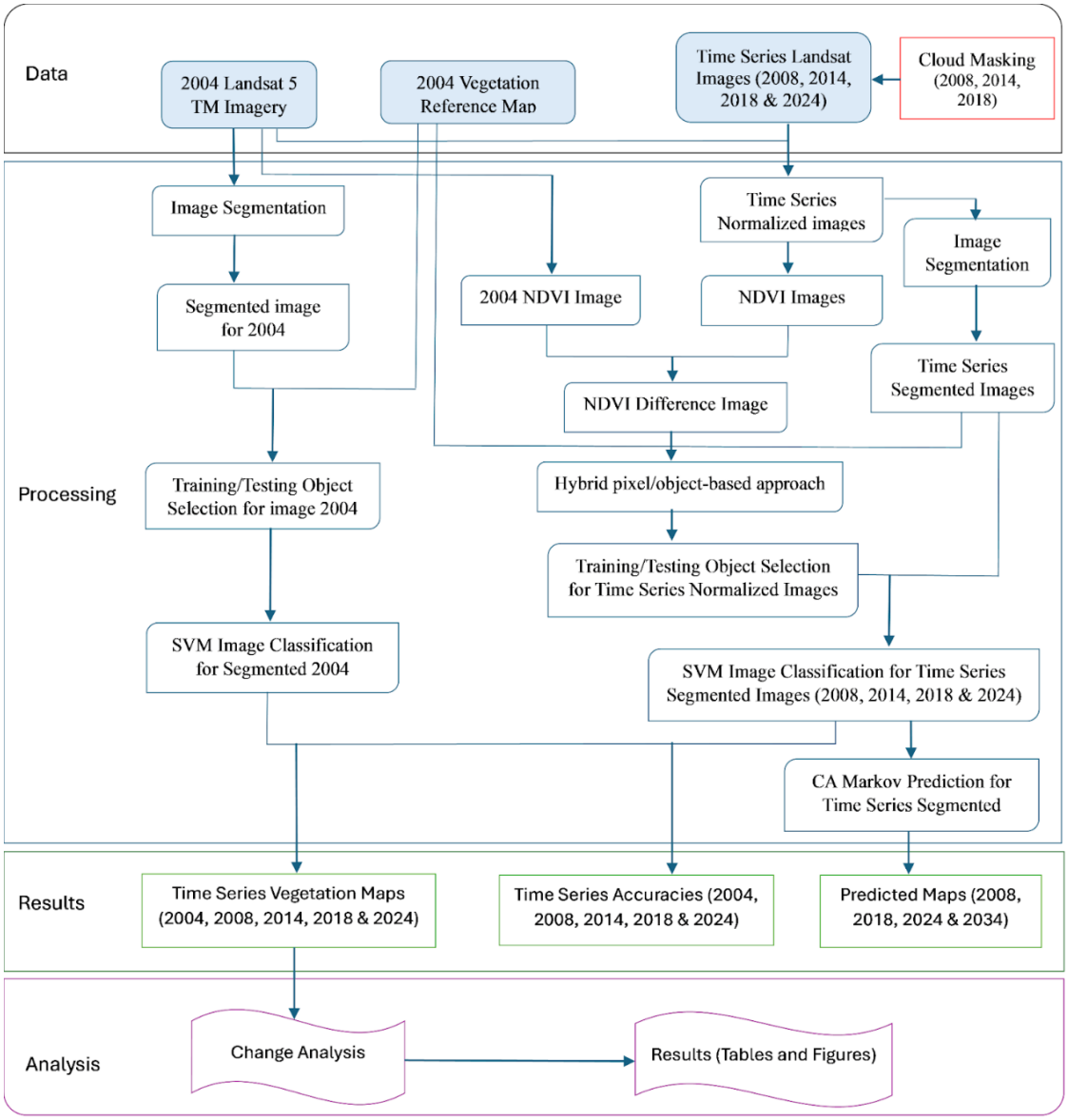

Figure 2. Methodological framework of the study.

3. Results

3.1. Vegetation Classification Results (2004–2024)

The time-series vegetation cover classification maps derived from the object-based SVM analysis (Figure 3) and the corresponding area estimates (Table 2) reveal clear spatiotemporal shifts in WCA-3A over the 20-year period. Sawgrass consistently dominated the landscape, covering about 69% of the area in 2004 and maintaining a strong presence of around 67% by 2024, despite intermediate fluctuations such as a drop to 63% in 2014 (Table 2). In contrast, Open Marsh areas showed pronounced dynamics, declining sharply from 23% in 2004 to just 11% by 2008, before recovering to nearly 24% in 2014 and expanding to about 27% by 2024.

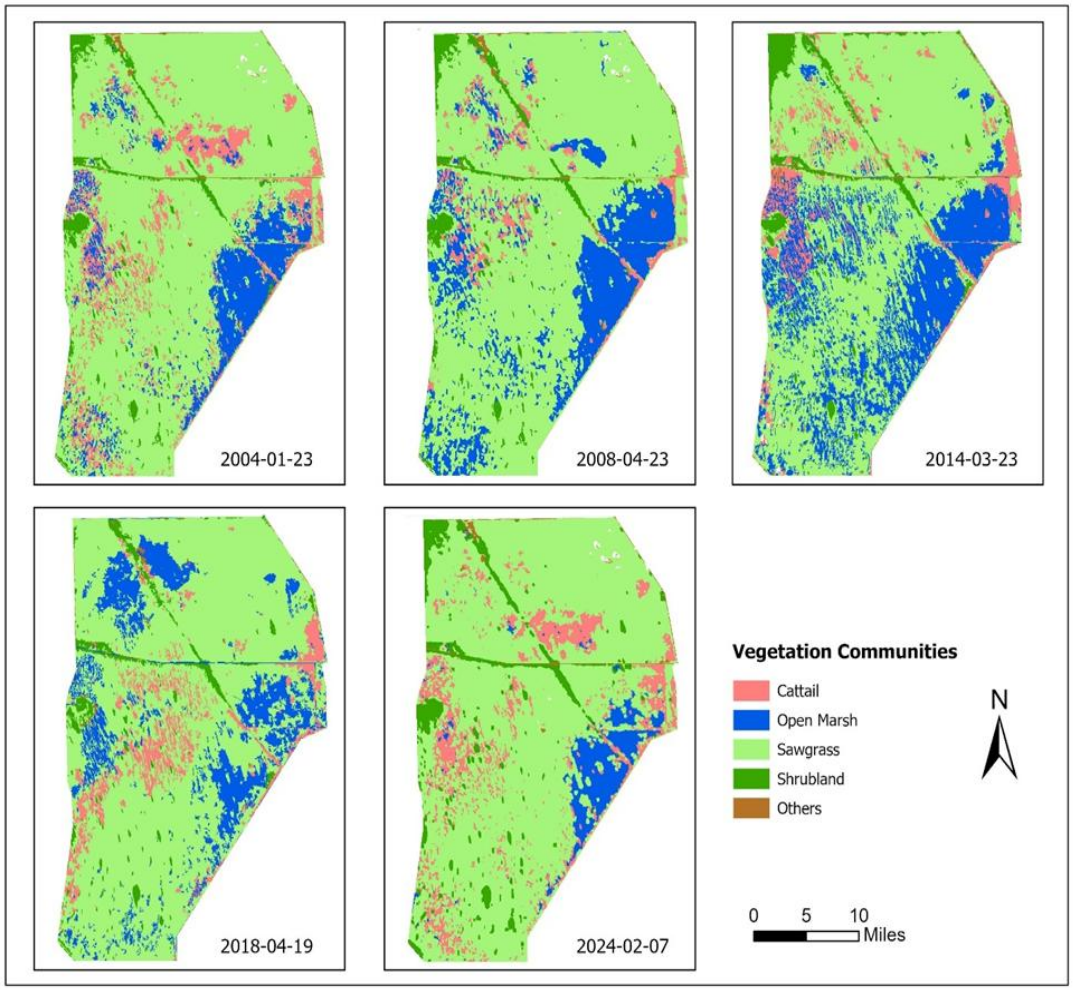

Figure 3. Object-based classification maps of vegetation communities in WCA-3A from 2004 to 2024 derived from Landsat imagery.

The invasive Cattail class experienced dramatic changes, expanding from about 5% in 2004 to over 11% by 2008, then steadily contracting to just 1.6% by 2024, largely persisting along the eastern and northeastern margins. Shrubland gradually increased along levees and canals, growing from 2% to over 4% by 2014 and remaining stable near that level by 2024. Meanwhile, the "Others" category, including bare ground, roads, and infrastructure, stayed negligible at under 1% throughout. Together, these trends highlight the dynamic interplay of vegetation communities, water levels, and ecosystem management shaping the long-term resilience and spatial heterogeneity of WCA-3A.

Table 2. Total area (ha) of vegetation communities in WCA-3A by class for each observation year (2004–2024) and projected 2034.

Date	Cattail	Open Marsh	Sawgrass	Shrubland	Others	Total
23 Jan 2004	9761	45587	135275	4423	976	196,023
23 Apr 2008	22326	21607	142916	7844	1023	195,716
23 Mar 2014	15125	47637	123080	9275	749	195,866
19 Apr 2018	14965	28970	143858	7336	889	196,019
07 Feb 2024	3114	52763	130849	8475	820	195,022
Projected 2034	1729	66116	117419	9535	1230	195,029

3.2. Vegetation Area Change

The spatial distribution of vegetation communities in WCA-3A highlights both temporal shifts and internal marsh heterogeneity. As shown in Figure 3 and detailed in Table 3, area changes for each class varied substantially across the study period. Figure 4 illustrates that Cattail experienced the largest fluctuations, with a marked expansion of 6.4% from 2004 to 2008 but a steady decline thereafter, ending with a net reduction of about 3.4% by 2024. Open Marsh showed the opposite trend, initially losing 12.2% during 2004–2008, yet recovering in later periods to achieve an overall net gain of 3.7%. Sawgrass exhibited only a modest net decline over two decades by 2024 despite being the dominant cover. Shrubland steadily expanded throughout, resulting in a cumulative gain of 2.0%, while the "Others" class remained nearly constant, changing by less than 0.1%. Together, these results (Table 3) emphasize the dynamic nature of wetland vegetation cover and the ecological processes driving change within the WCA-3A ecosystem.

Table 3. Land cover transition areas (ha) across time intervals (2004–2024) in WCA-3A, Florida Everglades. Values represent the total area of each class involved in transitions during each period.

Classes	2004–2008 Area (ha)	2008–2014 Area (ha)	2014–2018 Area (ha)	2018–2024 Area (ha)	2004–2024 Area (ha)
Cattail	12,564	7,201.30	159	11,851	6,647
Open Marsh	23,980	26,030	18,667	23,793	7,176
Sawgrass	7,641	19,836	20,778	13,009	4,426
Shrubland	3,421	1,431	1,939	1,139	4,052
Others	47	273	139	68	156

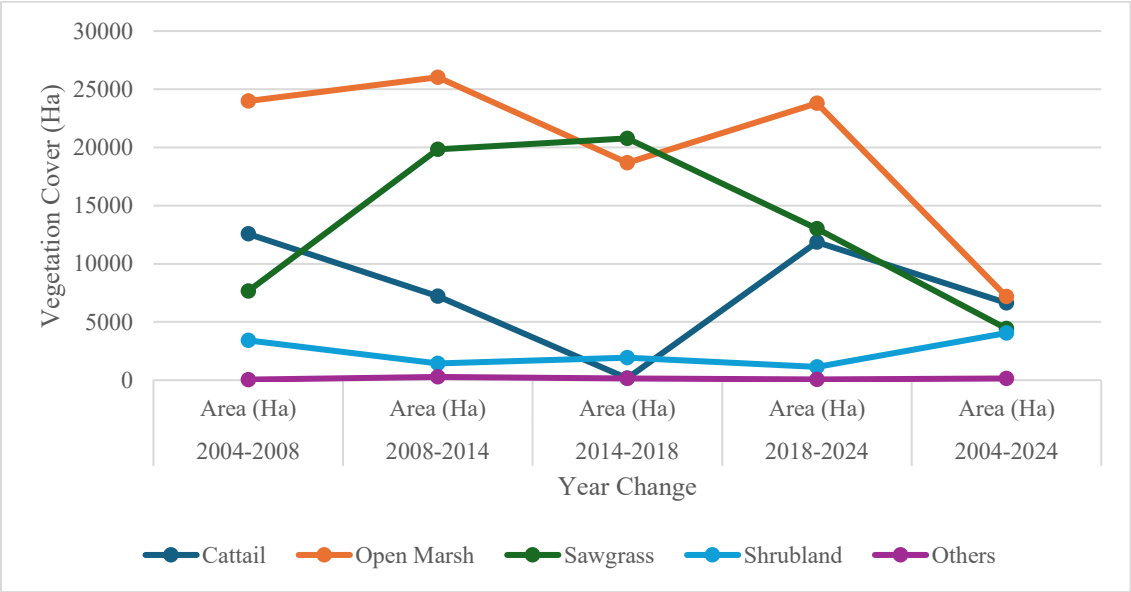

Figure 4. Temporal trends in vegetation cover (ha) for Cattail, Open Marsh, Sawgrass, Shrubland, and Others across four time intervals (2004–2024).

3.3. Classification Accuracy and Validation Results

To validate the object-based SVM classification results, an accurate assessment was performed for each step using independent reference data (Table 4). Overall classification accuracy was consistently high, ranging from 90% to 93%, with corresponding kappa coefficients between 0.80 and 0.87. This indicates substantial agreement across all years. The highest accuracy was achieved for the 2004 Landsat 5 TM dataset (93%, kappa = 0.87), supported by high-quality reference maps and well-defined vegetation boundaries. Despite transitions among Landsat sensors (from Landsat 5 TM to Landsat 8 OLI and Landsat 9 OLI), the results demonstrate stable classifier performance and effective radiometric normalization across the entire multi-temporal series.

Per-class user's and producer's accuracies also remained robust. The dominant Sawgrass and Open Marsh classes consistently achieved both user's and producer's accuracies above 90%, reflecting their clear spectral separability and large spatial extents. Shrubland and "Others" classes showed acceptable performance, though with slightly greater variability due to their smaller and more fragmented distributions. The invasive Cattail class exhibited the greatest temporal variation in accuracy: producer's accuracy peaked at 90% in 2008, coinciding with its maximum spatial coverage, but dropped to 50% in 2024 as Cattail cover fragmented into narrow, mixed patches that are more challenging to detect using medium-resolution (30 m) imagery. This outcome aligns with previous findings on the limitations of detecting sparse or spectrally mixed vegetation types in object-based classifications (Blaschke, 2010; Lu and Weng, 2007; Wang et al., 2022).

Table 4. Classification accuracy assessment for object-based SVM vegetation classification in WCA-3A across five Landsat time points (2004–2024). Values reported for each class are Producer's Accuracy (P) and User's Accuracy (U), expressed as percentages (P/U %). Overall Accuracy and kappa statistics are also provided for each year based on the total number of validation samples.

Year	Overall Accuracy (%)	Kappa	Samples	Cattail P (%)	Cattail U (%)	Open Marsh P (%)	Open Marsh U (%)	Sawgrass P (%)	Sawgrass U (%)	Shrubland P (%)	Shrubland U (%)	Others P (%)	Others U (%)
2004	93	0.87	409	100	92	90	91	96	95	57	80	90	100
2008	91	0.82	508	92	84	67	94	99	92	73	69	100	100
2014	91	0.85	407	83	79	90	93	93	96	88	41	90	100
2018	91	0.81	509	83	93	76	86	97	92	80	75	80	100
2024	90	0.81	460	50	70	91	93	94	94	62	36	90	100

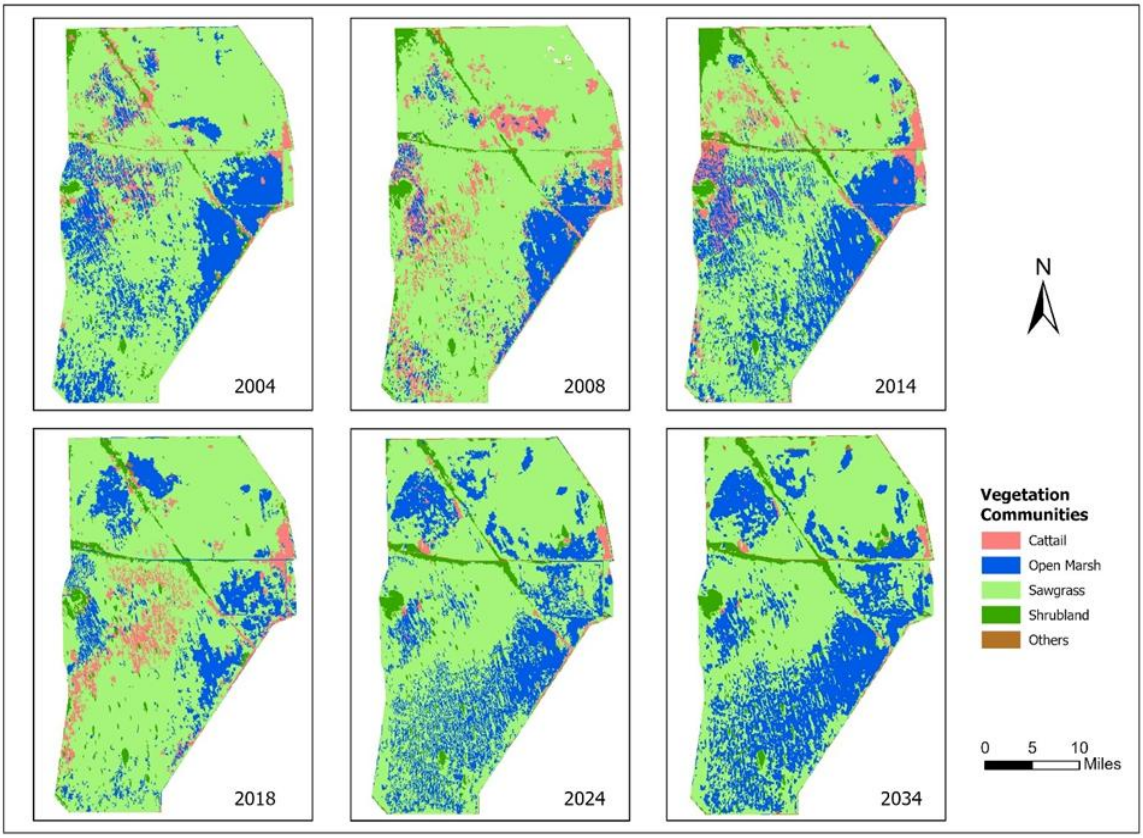

Figure 5. Temporal and predicted vegetation dynamics in WCA-3A (2004–2034).

3.4. Predicted Future Dynamics (2034)

Using the observed transition probabilities from 2004 to 2024, the Markov chain-based projection indicates continued recovery of native vegetation communities in WCA-3A by 2034 under current restoration trends (Figure 5). Cattail (*Typha spp.*) is predicted to substantially reduce further, shrinking from 3,114 ha in 2024 to approximately 1,729 ha (Table 2), representing less than 1% of the total marsh area. Sawgrass (*Cladium jamaicense*) is projected to maintain its dominance, gradually expanding to occupy over 70% of WCA-3A, as it continues to recolonize former cattail-dominated zones. Open Marsh, having expanded considerably during earlier restoration phases, is expected to stabilize with minor fluctuations in extent. Shrubland and "Others" classes are projected to remain relatively stable with minimal area change. The spatial distribution highlights that remaining cattail patches are likely to persist only along isolated fringes, while the broader landscape shifts toward a restored mosaic of sawgrass marsh and open water. These projections suggest that continued nutrient reduction and hydrologic restoration will likely drive WCA-3A closer to its historical ecosystem state by 2034.

4. Discussion

4.1. Vegetation Dynamics: Evidence for Effective Restoration

The time-series classification shows that sawgrass (*Cladium jamaicense*) has remained the dominant vegetation type across WCA-3A since 2004, covering roughly 69% of the area at the start of the study period and maintaining a strong presence of about 67% by 2024. Although this represents only a modest net decrease of about 2.3%, it is important to recognize that this persistence occurred despite decades of historical hydrologic alteration, nutrient enrichment, and pressures from invasive species. The resilience of sawgrass aligns with broader trends observed in other parts of the Everglades and comparable floodplain marshes where native graminoid dominance can be maintained if nutrient loading is reduced and natural hydroperiods are partially restored (Bernhardt and Willard, 2009; Bansal et al., 2019). In contrast, the open marsh community showed highly dynamic behavior, initially declining sharply from approximately 23% of the total area in 2004 to just 11% by 2008. This early loss likely reflects sustained high water levels and nutrient-induced vegetation encroachment, which promoted the expansion of more competitive species like cattail and sawgrass into formerly open-water patches. However, as restoration initiatives improved flow regimes and nutrient inputs were controlled, open marsh coverage rebounded significantly, rising to nearly 24% by 2014 and expanding further to about 27% in 2024, an overall net gain of 3.7% over two decades. This trajectory supports the view that open marsh communities can exhibit remarkable capacity for natural recovery once stressors are alleviated (Bartaloš et al., 2022; Wan et al., 2014).

The most striking trend is the dramatic expansion and subsequent decline of the invasive cattail (*Typha spp.*). Between 2004 and 2008, cattail area surged by 6.4%, nearly doubling to occupy more than 11% of WCA-3A. This peak coincides with legacy conditions of phosphorus enrichment and hydrological regimes that favor *Typha* expansion and competitive dominance over native sawgrass communities (Noe and Childers, 2007; Brix et al., 2010). However, continuous hydrologic improvements and nutrient control measures appear to have reversed this trend, with cattail coverage steadily shrinking to just 1.6% by 2024, an overall net decrease of about 3.4% across the study window. Such large-scale retraction is rarely documented in North American wetlands, underlining the effectiveness of integrated management. Similar success stories have been reported for *Phragmites australis* in the Great Lakes region, where sustained nutrient reduction and hydrologic variability helped suppress reinvasion (Lishawa et al., 2017). The spatial distribution maps further suggest that remaining cattail patches are confined to isolated margins near levees and canals, areas that require continued monitoring as potential reinvasion corridors.

Shrubland communities in WCA-3A exhibited a modest but steady increase, expanding by 2% over the study period. This is consistent with the tendency for woody shrubs to establish along levees, canal edges, and slightly elevated tree islands, microtopographic features that create drier conditions favoring shrub encroachment (Bernhardt et al., 2011). The "Others" class, which includes bare ground, roads, and built infrastructure, remained negligible throughout (<1%), highlighting the predominantly natural state of WCA-3A's vegetation cover despite decades of hydrological alteration.

4.2. Insights from Markov Chain Projection

Using the observed transition probabilities from 2004–2024, the Markov chain projection to 2034 suggests that WCA-3A is on a positive ecological trajectory under continued restoration. Cattail cover is projected to decline further to less than 1% of total area, shrinking from 3,114 ha in 2024 to around 1,729 ha by 2034. Meanwhile, sawgrass is forecast to expand slightly, potentially reclaiming over 70% of the marsh. Open Marsh is expected to stabilize with only minor fluctuations, and Shrubland and "Others" classes are projected to remain steady. This projection reinforces the principle that tackling root causes, such as nutrient loading and unnatural hydrological regimes, is more sustainable than repeated mechanical removal alone (Tuchman et al., 2009; Simberloff et al., 2013). However, it also aligns with international lessons that caution trajectories may be fragile if management intensity wanes (Bartaloš et al., 2022; Paynter and Flanagan, 2004).

4.3. Methodological Contributions and Limitations

The classification results demonstrate strong and consistent performance, with overall accuracies exceeding 90% and kappa coefficients ranging from 0.80 to 0.87 across all years. These results underscore the value of integrating OBIA with SVM classification for capturing long-term vegetation dynamics in large wetland systems using moderate-resolution satellite imagery. Consistent with previous studies (Blaschke, 2010; Pande-Chhetri et al., 2017), the object-based framework effectively reduced salt-and-pepper noise and improved class coherence within heterogeneous marsh mosaics. The use of multiresolution segmentation and contextual texture features likely contributed to the high producer's and user's accuracies observed for dominant vegetation classes such as sawgrass and open marsh, which remained above 90% in most years.

However, producer's accuracy for cattail declined in later years, reaching approximately 50% in 2024. This estimate was based on a relatively small number of validation samples (n = 14). As cattail became increasingly rare and spatially fragmented, fewer reference points were available for accuracy assessment. The limited sample size amplifies the sensitivity of producer accuracy to individual misclassifications and partially reflects the declining prevalence of cattail within WCA-3A. Moreover, remaining *Typha* stands were largely confined to narrow levee margins and edge zones, where moderate-resolution (30 m) imagery may under-detect mixed or transitional pixels. While small residual patches may therefore be underestimated, the substantial landscape-scale reduction in cattail coverage is supported by consistent multi-temporal trends and independent validation results.

These findings align with established limitations of medium-resolution imagery for detecting narrow, fragmented, or spectrally mixed vegetation stands (Blaschke et al., 2014; Wang et al., 2022). Small patches along levee margins may remain undetected or misclassified, potentially leading to underestimation of localized reinvasion. Integrating higher-resolution UAV or Sentinel-2 imagery within object-based frameworks could improve early detection of subtle regrowth and edge dynamics (Pande-Chhetri et al., 2017). Furthermore, coupling finer-resolution mapping with spatially explicit transition models, such as CA-Markov simulations, may better capture local-scale drivers, including canal proximity and micro-topographic variation (Tahir et al., 2025).

Finally, the consistent classification performance across sensor transitions from Landsat 5 TM to Landsat 8 OLI and Landsat 9 OLI highlights the effectiveness of the radiometric normalization and cross-validation procedures applied in this study. Maintaining classification stability across multiple sensor generations strengthens confidence in the temporal comparability of the 2004–2024 vegetation time series and demonstrates the robustness of the workflow for long-term monitoring applications (Erfanifard et al., 2022).

4.4. Management Implications and Future Directions

The strong evidence for Cattail declines and native community recovery in WCA-3A underlines that large-scale wetland restoration can succeed when informed by integrated data and adaptive management. The observed expansion of Open Marsh, alongside stable or recovering Sawgrass dominance, supports the idea that diversifying hydroperiods and reducing nutrient inputs can promote more complex, resilient native mosaics (Osland et al., 2011; Lishawa et al., 2017). Yet, caution is warranted. Edge effects, especially near canals and levees, remain hotspots for reinvasion, as confirmed by the moderate increase in Shrubland cover in those areas. This mirrors findings from Everglades tree island studies, which show that microtopographic and hydrological variability must be maintained to prevent shrub encroachment and invasive dominance (Bernhardt and Willard, 2009). Our results reinforce the importance of long-term monitoring, especially of these vulnerable fringe areas.

Methodologically, this study illustrates that while Landsat's long archive and free access make it invaluable for decadal-scale trend detection, supplementing moderate-resolution imagery with finer-scale data is critical for adaptive management. The synergy of OBIA and higher-resolution UAV or Sentinel-2 imagery could enable near-real-time mapping of incipient patches, a significant leap forward for early detection and rapid response (Pande-Chhetri et al., 2017; Wang et al., 2022).

Finally, the Markov projection underscores the usefulness of scenario-based modeling for informing restoration planning. However, future work should expand this by integrating local-scale hydrological and biogeochemical models to refine transition probabilities, particularly in the face of climate-induced hydrological extremes.

5. Conclusions

This study demonstrates that integrating a multi-decadal Landsat time series with OBIA and SVM classification provides a reliable framework for tracking long-term vegetation dynamics in large, heterogeneous wetland systems. In WCA-3A, the results indicate that sustained hydrological restoration and nutrient reduction have altered vegetation trajectories over the past two decades. The marked reduction in invasive Cattail cover, the rebound and stabilization of Open Marsh communities, and the continued dominance of native Sawgrass collectively suggest that addressing underlying drivers, particularly nutrient loading and altered hydroperiods, supports durable ecosystem recovery. These findings align with broader evidence that integrated restoration strategies can suppress invasive monocultures and promote resilient native vegetation structure.

Consistently high classification accuracies (>90%) across multiple Landsat sensors confirm the robustness of the OBIA-SVM approach for decadal-scale monitoring using moderate-resolution imagery. The Markov-based projection further demonstrates how historical classification outputs can be translated into near-term scenario assessments to support adaptive management. At the same time, the persistence of small cattail patches and localized shrub expansion near levee margins indicates that edge environments remain vulnerable and require continued monitoring.

Future efforts should integrate higher-resolution imagery, such as Sentinel-2 or UAV data, to improve detection of fragmented or early-stage reinvasion. Incorporating spatially explicit transition models that account for hydrological variability and micro-topographic drivers would further strengthen predictive capacity. As wetlands face increasing climatic and anthropogenic pressures, combining long-term Earth observation with adaptive modeling approaches will remain essential for informed restoration planning and sustained ecosystem resilience.

Funding: The authors declare that no funds, grants, or other support were received during the preparation of this manuscript.

Data Availability Statement: The datasets generated and analyzed during the study will be made available by the corresponding author upon reasonable request

Acknowledgment: The authors thank the editor and anonymous reviewers for their constructive comments, which helped improve the quality and clarity of this manuscript.

Conflicts of Interest: The authors declare no conflicts of interest.

References

Bansal, S., Lishawa, S. C., Newman, S., Tangen, B. A., Wilcox, D., Albert, D., Anteau, M. J., Chimney, M. J., Cressey, R. L., DeKeyser, E., Lawrence, B. A., Nurminen, L., Reo, N. J., Richards, J., Rodgers, L., Shalvey, N., and Windham-Myers, L. (2019). *Typha* (cattail) invasion in North American wetlands: Biology, regional problems, impacts, ecosystem services, and management. *Wetlands***,** 39, 645–684. https://doi.org/10.1007/s13157-019-01174-7

Bartaloš, T., Bruna, J., Dvořák, P., and Müllerová, J. (2022). Object-based image analysis for monitoring plant invasions: Can we use an open-source solution? *Remote Sensing*, 14(21), 5506. https://doi.org/10.5281/zenodo.7290188

Belanger, T. V., Scheidt, D. J., and Platko, J. R. (2009). Effects of nutrient enrichment on the Florida Everglades. *Environmental Management*, 5(1), 101–111. https://doi.org/10.1080/07438148909354686

Bernhardt, C. (2011). Native Americans, regional drought and tree island evolution in the Florida Everglades. *The Holocene*, *21*(6), 967-978. https://doi.org/10.1177/0959683611400204

Bernhardt, C. E., and Willard, D. A. (2009). Response of the Everglades ridge and slough landscape to climate variability and 20th-century water management. *Ecological applications: a publication of the Ecological Society of America*, *19*(7), 1723–1738. https://doi.org/10.1890/08-0779.1

Blaschke, T. (2010). Object based image analysis for remote sensing. *ISPRS Journal of Photogrammetry and Remote Sensing,* 65(1), 2–16. https://doi.org/10.1016/j.isprsjprs.2009.06.004

Blaschke, T., Hay, G. J., Kelly, M., Lang, S., Hofmann, P., Addink, E., Feitosa, R. Q., van der Meer, F., van der Werff, H., van Coillie, F., and Tiede, D. (2014). Geographic object-based image analysis: Towards a new paradigm. *ISPRS Journal of Photogrammetry and Remote Sensing, 87*, 180–191. https://doi.org/10.1016/j.isprsjprs.2013.09.014

Brix, H., Lorenzen, B., Mendelssohn, I. A., McKee, K. L., and Miao, S. (2010). Can differences in phosphorus uptake kinetics explain the distribution of cattail and sawgrass in the Florida Everglades? *BMC Plant Biology, 10*, 23. https://doi.org/10.1186/1471-2229-10-23

Cui, L., Li, G., Chen, Y., and Li, L. (2021). Response of landscape evolution to human disturbances in the coastal wetlands in northern Jiangsu Province, China. *Remote Sensing*, 13(11), 2030.https://doi.org/10.3390/rs13112030

Davis, S. M., and Ogden, J. C. (1994). *Everglades: The Ecosystem and Its Restoration*. St. Lucie Press.

Entry, J. A., and Gottlieb, A. (2014). The impact of stormwater treatment areas and agricultural best management practices on water quality in the Everglades Protection Area. *Environmental Monitoring and Assessment*, 186(2), 1023–1037. https://doi.org/10.1007/s10661-013-3436-4

Erfanifard, Y., Nasirabad, M. L., and Stereńczak, K**.** (2022). Assessment of Iran's mangrove forest dynamics (1990–2020) using Landsat time series. *Remote Sensing*, 14(19), 4912. https://doi.org/10.3390/rs14194912

Finkl, C.W., Makowski, C. (2017). The Florida Everglades: An Overview of Alteration and Restoration. In: Finkl, C., Makowski, C. (eds) Coastal Wetlands: Alteration and Remediation. *Coastal Research Library*, vol 21. Springer, Cham. https://doi.org/10.1007/978-3-319-56179-0_1

Hestir, E. L., Khanna, S., Andrew, M. E., Santos, M. J., Viers, J. H., Greenberg, J. A., Rajapakse, S. S., and Ustin, S. L. (2008). Identification of invasive vegetation using hyperspectral remote sensing in the California Delta ecosystem. *Remote Sensing of Environment*, 112(11), 4034–4047. https://doi.org/10.1016/j.rse.2008.01.022

Kanjin, K., and Alam, B. M. (2024). Assessing changes in land cover, NDVI, and LST in the Sundarbans mangrove forest in Bangladesh and India: A GIS and remote sensing approach. *Remote Sensing Applications: Society and Environment*, 36, 101289. https://doi.org/10.1016/j.rsase.2024.101289

Lagerwall, G., Kiker, G. A., Muñoz-Carpena, R., Convertino, M., James, A. I., and Wang, N. (2012). A spatially distributed, deterministic approach to modeling *Typha Typha spp.* (cattail) in an Everglades wetland. *Ecological Processes*, 1(1), 10. https://doi.org/10.1186/2192-1709-1-10

Lishawa SC, Carson BD, Brandt JS, Tallant JM, Reo NJ, Albert DA, Monks AM, Lautenbach JM and Clark E (2017) Mechanical harvesting effectively controls young *Typha spp.* invasion and unmanned aerial vehicle data enhances post-treatment monitoring. *Frontiers in Plant Science*, 8:619. https://doi.org/10.3389/fpls.2017.00619

Lu, D., and Weng, Q. (2007). A survey of image classification methods and techniques for improving classification performance. *International Journal of Remote Sensing*, 28(5), 823–870. https://doi.org/10.1080/01431160600746456.

Mountrakis, G., Im, J., and Ogole, C. (2011). Support vector machines in remote sensing: A review. *ISPRS Journal of Photogrammetry and Remote Sensing, 66*(3), 247–259. https://doi.org/10.1016/j.isprsjprs.2010.11.001

Noe, G. B., and Childers, D. L. (2007). Phosphorus budgets in Everglades wetland ecosystems: The effects of hydrology and nutrient enrichment. *Wetlands Ecology and Management, 15*(3), 189–205. https://doi.org/10.1007/s11273-006-9023-5

Osland, M. J., González, E., Richardson, C. J., and Dahm, C. N. (2011). Restoring diversity after cattail expansion: Disturbance, resilience, and seasonality in a tropical dry wetland. *Ecological Applications, 21*(3), 715–728. https://doi.org/10.1890/09-0981.1

Pal, M., and Mather, P. M. (2005). Support vector machines for classification in remote sensing. *International Journal of Remote Sensing*, *26*(5), 1007–1011. https://doi.org/10.1080/01431160512331314083

Pande-Chhetri, R., Abd-Elrahman, A., Liu, T., Morton, J., and Wilhelm, V. L. (2017). Object-based classification of wetland vegetation using very high-resolution unmanned air system imagery. *European Journal of Remote Sensing*, *50*(1), 564–576. https://doi.org/10.1080/22797254.2017.1373602

Paynter, Q., Flanagan, G. J. (2004). Integrated weed management: Could we be doing better? Lessons from controlling the invasive wetland shrub, Mimosa pigra. *In Proceedings of the 14th Australian Weeds Conference* (pp. 361–369). https://www.invasive.org/proceedings/pdfs/11_361-369.pdf

Reis, V., Hermoso, V., Hamilton, S. K., Ward, D., Fluet-Chouinard, E., Lehner, B., and Linke, S. (2017). A global assessment of inland wetland conservation status. *Bioscience*, 67(6), 523-533. https://doi.org/10.1093/biosci/bix045

Rodgers, L., Pernas, T., Redwine, J., Shamblin, B., and Bruscia, S. (2018). Multiscale invasive plant monitoring: Experiences from the Greater Everglades Restoration Area. *Weed Technology*, 32(1), 11–19. https://doi.org/10.1017/WET.2017.106

Sandhya, G., Nandy, S., Padalia, H., Dey, A., Nath, A. J., Majumdar, K., and Das, A. K. (2025). Unveiling the spatio-temporal dynamics of Son Beel: A freshwater wetland from Indian East Sub-Himalaya. *Journal of the Indian Society of Remote Sensing*. Advance online publication. https://doi.org/10.1007/s12524-025-02201-3

Simberloff, D., Martin, J.-L., Genovesi, P., Maris, V., Wardle, D. A., Aronson, J., Courchamp, F., Galil, B., García-Berthou, E., Pascal, M., Pyšek, P., Sousa, R., Tabacchi, E., and Vilà, M. (2013). Impacts of biological invasions: What's what and the way forward. *Trends in Ecology* and *Evolution*, 28(1), 58–66. https://doi.org/10.1016/j.tree.2012.07.013

South Florida Ecosystem Restoration Task Force. (n.d.). *Water quality programs*. https://www.evergladesrestoration.gov/water-quality-programs

South Florida Water Management District (SFWMD). (n.d.). *Water quality improvement and stormwater treatment areas (STAs)*. https://www.sfwmd.gov/our-work/wq-stas

Stepchenko, A., and Chizhov, J. (2015). Applying Markov chains for NDVI time series forecasting of Latvian regions. *Information Technology and Management Science*, 18(1), 57–61. https://doi.org/10.1515/itms-2015-0009

Tahir, Z., Haseeb, M., Mahmood, S. A., et al. (2025)**.** Predicting land use and land cover changes for sustainable land management using CA-Markov modelling and GIS techniques. *Scientific Reports, 15*, 3271. https://doi.org/10.1038/s41598-025-87796-w

Tuchman, N. C., Larkin, D. J., Geddes, P., Wildova, R., Jankowski, K., and Goldberg, D. E. (2009). Patterns of environmental change associated with *Typha* xglauca invasion in a Great Lakes coastal wetland. *Wetlands*, 29(3), 964–975. https://doi.org/10.1672/08-71.1

Wan, H., Wang, Q., Jiang, D., Fu, J., Yang, Y., and Liu, X. (2014). Monitoring the invasion of Spartina alterniflora using very high resolution unmanned aerial vehicle imagery in Beihai, Guangxi (China). *The Scientific World Journal*, *2014*, 638296. https://doi.org/10.1155/2014/638296

Wang, Z., Wei, C., Liu, X., Zhu, L., Yang, Q., Wang, Q., … Meng, Y. (2022). Object-based change detection for vegetation disturbance and recovery using Landsat time series. *GIScience& Remote Sensing*, *59*(1), 1706–1721. https://doi.org/10.1080/15481603.2022.2129870

Willard, D. A., and Bernhardt, C. E. (2011). Impacts of past climate and sea level change on Everglades wetlands: placing a century of anthropogenic change into a late-Holocene context. *Climatic Change*, 107(1), 59-80. https://doi.org/10.1007/s10584-011-0078-9

Yankyera, S., and Alam, B. M. (2025). Five decades of transformation due to human-environment stressors: Land cover, vegetation, and land surface temperature change analysis in the largest wetland ecosystem in Bangladesh. *Earth Systems and Environment,* 9(1), 589–604. https://doi.org/10.1007/s41748-025-00652-9

Yeoman, K., Jiang, B., and Mitsch, W. J. (2017). Phosphorus concentrations in a Florida Everglades water conservation area before and after El Niño events in the dry season. *Ecological Engineering,* 99, 206–215. https://doi.org/10.1016/j.ecoleng.2017.07.028.

Zhang, C., Smith, M., Lv, J., and Fang, C. (2017). Applying time series Landsat data for vegetation change analysis in the Florida Everglades Water Conservation Area 2A during 1996–2016. *International Journal of Applied Earth Observation and Geoinformation*, 57, 214–223. https://doi.org/10.1016/j.jag.2017.01.007

Disclaimer/Publisher's Note: The statements, opinions and data contained in all publications are solely those of the individual author(s) and contributor(s) and not of JEOGA or the editor(s). JEOGA or the editor(s) disclaim responsibility for any injury to people or property resulting from any ideas, methods, instructions or products referred to in the content.

APPENDIX A

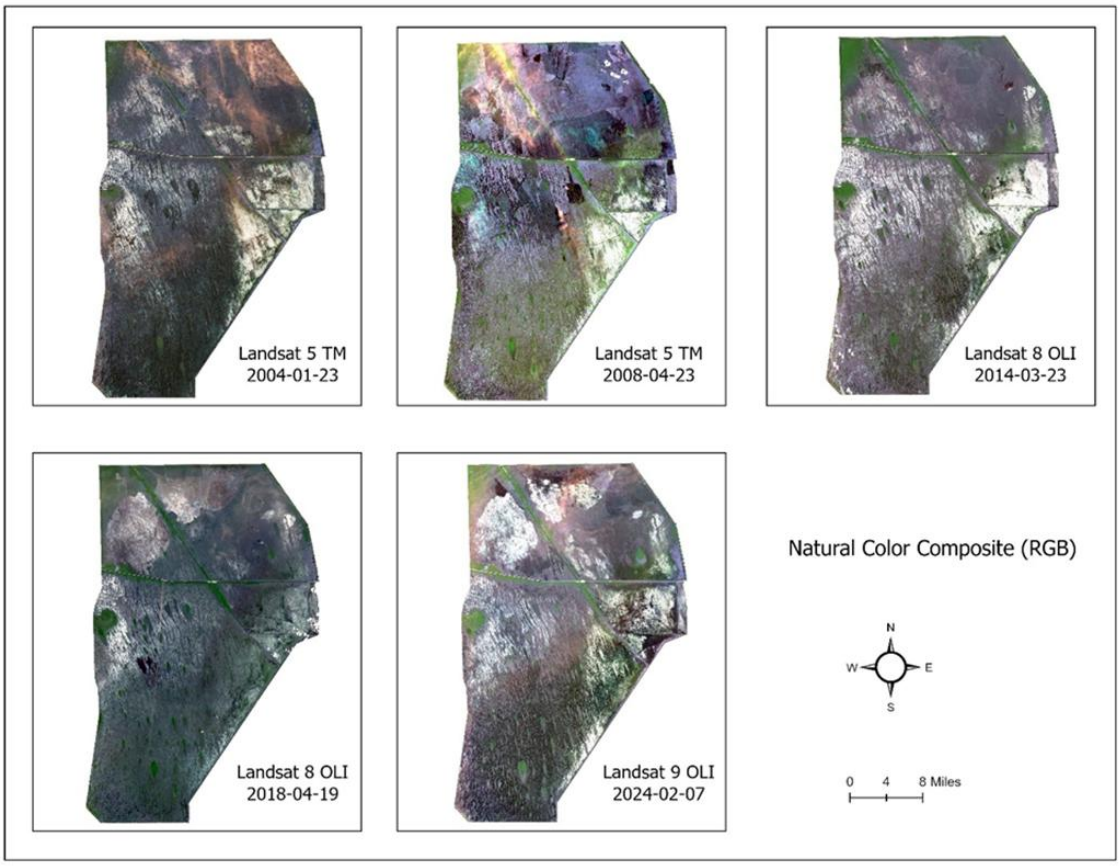

Figure A1. Natural Color composite of Landsat images for 2004–2024. This figure presents natural color composite (RGB) images of WCA-3A from Landsat 5 TM (2004, 2008), Landsat 8 OLI (2014, 2018), and Landsat 9 OLI (2024).

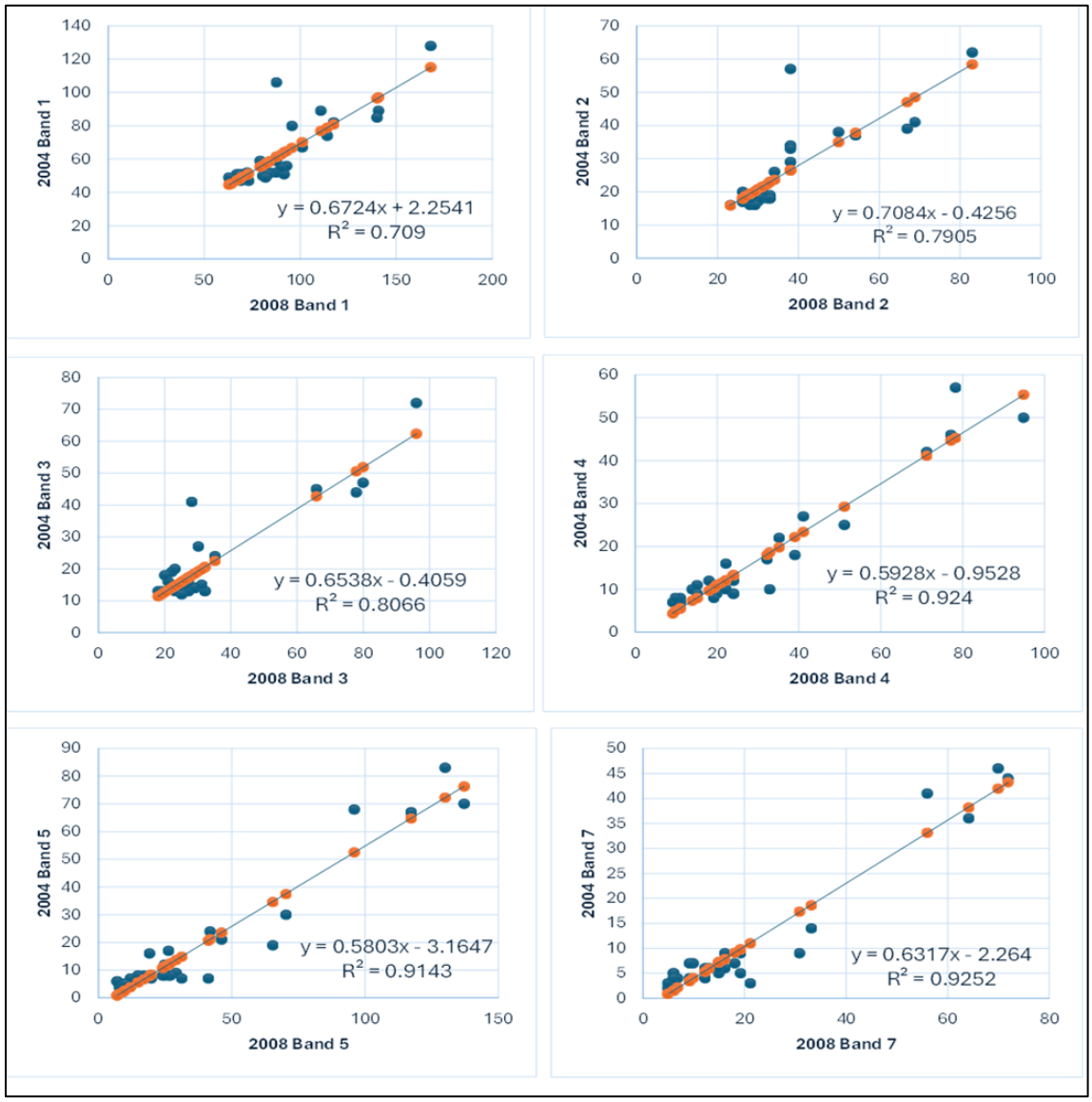

Figure A2. Pseudo-invariant feature (PIF) regression relationships for radiometric normalization of 2004 and 2008 Landsat bands.

This figure shows the relationship between PIFs in the 2004 and 2008 Landsat images across bands 1–7. The scatter plots illustrate linear regression trends, with high R^2 values (0.709–0.925) indicating strong correlations between the two years. This suggests that PIFs remained stable, confirming their suitability for radiometric normalization. Variations in regression slopes reflect differences in sensor characteristics or atmospheric conditions, ensuring that observed vegetation changes are due to actual land cover dynamics rather than sensor inconsistencies.

Table A1. Equations used for the normalization of the other images, using 2004 as the base image.

Date and Sensor	Band	Equation	R^2	PIFs
23 Apr 2008 Landsat-5 TM	Band 1 Band 2 Band 3 Band 4 Band 5 Band 7	y = 0.6724x + 2.2541 y = 0.7084x - 0.4256 y = 0.6538x - 0.4059 y = 0.5928x - 0.9528 y = 0.5803x - 3.1647 y = 0.6317x - 2.264	0.709 0.7905 0.8066 0.924 0.9143 0.9252	29
23 Mar 2014 Landsat -8 OLI	Band 2 Band 3 Band 4 Band 5 Band 6 Band 7	y = 0.011x – 40.737 y = 0.0049x - 14.745 y = 0.0054x - 19.475 y = 0.0038x - 13.116 y = 0.0063x - 26.48 y = 0.0047x - 19.731	0.4907 0.5029 0.7262 0.8128 0.9203 0.9238	30
19 Apr 2018 Landsat -8 OLI	Band 2 Band 3 Band 4 Band 5 Band 6 Band 7	y = 0.0046x + 14.366 y = 0.0022x + 4.603 y = 0.0025x - 1.5075 y = 0.0019x - 2.1089 y = 0.0029x - 7.9334 y = 0.0024x - 8.2923	0.3846 0.4365 0.7501 0.8538 0.8137 0.8385	29
07 Feb 2024 Landsat-9 OLI	Band 2 Band 3 Band 4 Band 5 Band 6 Band 7	y = 0.0028x + 37.992 y = 0.0019x + 9.9119 y = 0.0024x + 2.2762 y = 0.0023x - 1.7745 y = 0.0043x - 13.439 y = 0.0036x - 13.621	0.5033 0.6208 0.4945 0.4832 0.5815 0.6582	30

Table A2. Confusion matrices and class-specific accuracy metrics for object-based SVM classification across five Landsat time points (2004-2024) in WCA-3A.

2004

ClassValue	Cattail	Open Marsh	Sawgrass	Shrubland	Others	Total	U_Accuracy	Kappa
Cattail	22	1	1	0	0	24	0.916667	
Open Marsh	0	105	10	0	0	115	0.913043	
Sawgrass	0	10	241	2	1	256	0.941406	
Shrubland	0	0	1	4	0	5	0.8	
Others	0	0	0	0	9	9	1	
Total	22	116	253	6	10	409	0	
P_Accuracy	1	0.913043	0.956349	0.666667	0.9	0	0.93154	
Kappa								0.871175

2008

ClassValue	Cattail	Open Marsh	Sawgrass	Shrubland	Others	Total	U_Accuracy	Kappa
Cattail	56	4	4	0	0	64	0.84375	
Open Marsh	1	58	1	2	0	62	0.935484	
Sawgrass	3	20	330	3	0	356	0.918539	
Shrubland	1	3	0	11	0	16	0.6875	
Others	0	0	0	0	10	10	1	
Total	61	85	335	16	10	508	0	
P_Accuracy	0.915254	0.682353	0.98494	0.733333	1	0	0.905512	
Kappa								0.813129

2014

ClassValue	Cattail	Open Marsh	Sawgrass	Shrubland	Others	Total	U_Accuracy	Kappa
Cattail	33	4	3	0	1	42	0.785714	
Open Marsh	1	108	7	0	0	116	0.931034	
Sawgrass	4	5	213	1	0	223	0.955157	
Shrubland	2	3	5	7	0	17	0.411765	
Others	0	0	0	0	9	9	1	
Total	40	120	228	8	10	407	0	
P_Accuracy	0.825	0.9	0.934211	0.875	0.9	0	0.909091	
Kappa								0.847857

2018

ClassValue	Cattail	Open Marsh	Sawgrass	Shrubland	Others	Total	U_Accuracy	Kappa
Cattail	39	0	1	1	0	42	0.928571	
Open Marsh	3	68	7	0	1	79	0.860759	
Sawgrass	5	21	340	2	0	368	0.923913	
Shrubland	0	1	3	12	0	16	0.75	
Others	0	0	0	0	4	4	1	
Total	47	90	351	15	5	509	0	
P_Accuracy	0.829787	0.755556	0.968661	0.8	0.8	0	0.909627	
Kappa								0.805804

2024

ClassValue	Cattail	Open Marsh	Sawgrass	Shrubland	Others	Total	U_Accuracy	Kappa
Cattail	7	2	1	0	0	10	0.7	
Open Marsh	2	127	6	0	1	138	0.92029	
Sawgrass	4	7	261	5	0	281	0.928826	
Shrubland	1	3	9	8	0	22	0.363636	
Others	0	0	0	0	9	9	1	
Total	14	139	277	13	10	460	0	
P_Accuracy	0.5	0.913669	0.942238	0.615385	0.9	0	0.895652	
Kappa								0.806426